Chapter 7

Profile Monitoring with Nonlinear Mixed Models

Once the profiles are obtained, we propose to fit them with separate NL models or with a NLM model. The NLM model has the advantage of pooling information from the profiles together and allows us to model the random effects. When utilizing the NL approach, that of fitting separate NL regression models to each profile, we have reduced the profiles to a series of time-ordered vectors, $\widehat{\boldsymbol{\theta}_i}$. For the NLM model we have reduced the profiles to the estimated fixed effects vector, $\widehat{\boldsymbol{\theta}}$, and the vectors containing the estimated random deviations from the fixed effects vector, $\widehat{\mathbf{b}}_i$.

7.1 T^2 Statistic for NL and NLM models

The T^2 statistic will be similar to those in (5.2) and (5.5) with the parameter estimators of the NL and NLM approaches in place of those used for the LS and LMM approaches.

For the NL approach we use the $\widehat{\boldsymbol{\theta}_i}$ vectors to calculate the T^2 statistics. The T^2 statistic for the separate NL regression models based on the sample mean vector and variance-

covariance matrix is denoted by $T^2_{1,i,NL}$ and the T^2 statistic based on successive differences by $T^2_{2,i,NL}$. They are given by

$$\begin{aligned} T^2_{1,i,NL} &= (\widehat{\boldsymbol{\theta}}_{\boldsymbol{i}} - \overline{\boldsymbol{\theta}}_{\boldsymbol{i}})' \mathbf{S}^{-1}_{1,NL} (\widehat{\boldsymbol{\theta}}_{\boldsymbol{i}} - \overline{\boldsymbol{\theta}}_{\boldsymbol{i}}) \\ &= (\widehat{\boldsymbol{\theta}}_{\boldsymbol{i}} - \overline{\boldsymbol{\theta}}_{\boldsymbol{i}})' \left[\frac{\sum_{i=1}^{m} (\widehat{\boldsymbol{\theta}}_{\boldsymbol{i}} - \overline{\boldsymbol{\theta}}_{\boldsymbol{i}})(\widehat{\boldsymbol{\theta}}_{\boldsymbol{i}} - \overline{\boldsymbol{\theta}}_{\boldsymbol{i}})'}{m-1} \right]^{-1} (\widehat{\boldsymbol{\theta}}_{\boldsymbol{i}} - \overline{\boldsymbol{\theta}}_{\boldsymbol{i}}) \text{ for } i = 1, 2, \ldots, m, \quad (7.1) \end{aligned}$$

where

$$\overline{\boldsymbol{\theta}}_{\boldsymbol{i}} = \frac{\sum_{i=1}^{m} \widehat{\boldsymbol{\theta}}_{\boldsymbol{i}}}{m}, \quad (7.2)$$

and by

$$\begin{aligned} T^2_{2,i,NL} &= (\widehat{\boldsymbol{\theta}}_{\boldsymbol{i}} - \overline{\boldsymbol{\theta}}_{\boldsymbol{i}})' \mathbf{S}^{-1}_{2,NL} (\widehat{\boldsymbol{\theta}}_{\boldsymbol{i}} - \overline{\boldsymbol{\theta}}_{\boldsymbol{i}}) \\ &= (\widehat{\boldsymbol{\theta}}_{\boldsymbol{i}} - \overline{\boldsymbol{\theta}}_{\boldsymbol{i}})' \left[\frac{\sum_{i=1}^{m-1} (\widehat{\boldsymbol{\theta}}_{\boldsymbol{i+1}} - \widehat{\boldsymbol{\theta}}_{\boldsymbol{i}})(\widehat{\boldsymbol{\theta}}_{\boldsymbol{i+1}} - \widehat{\boldsymbol{\theta}}_{\boldsymbol{i}})'}{m-1} \right]^{-1} (\widehat{\boldsymbol{\theta}}_{\boldsymbol{i}} - \overline{\boldsymbol{\theta}}_{\boldsymbol{i}}) \text{ for } i = 1, 2, \ldots, m. \quad (7.3) \end{aligned}$$

Because the fixed effects vector, $\widehat{\boldsymbol{\theta}}$, is the same for all profiles in the NLM model, the T^2 statistic will only depend on the predicted random effects. In the NLM model the obtained eblups will rarely sum to zero but nonetheless, it can be shown by a proof similar to that of Theorem C.2 of Appendix C that the T^2 statistics based on the NLM model will only depend on the eblups.

The T^2 statistic based on the NLM model will be denoted by $T^2_{1,i,NLMM}$ and $T^2_{2,i,NLMM}$ and are respectively,

$$T^2_{1,i,NLMM} = (\widehat{\mathbf{b}}_i - \overline{\mathbf{b}})' \left[\frac{\sum_{i=1}^{m} (\widehat{\mathbf{b}}_i - \overline{\mathbf{b}})'(\widehat{\mathbf{b}}_i - \overline{\mathbf{b}})}{m-1} \right]^{-1} (\widehat{\mathbf{b}}_i - \overline{\mathbf{b}}) \text{ for } i = 1, 2, \ldots, m, \quad (7.4)$$

and

$$T^2_{2,i,NLMM} = (\widehat{\mathbf{b}}_i - \overline{\mathbf{b}})' \left[\frac{\sum_{i=1}^{m-1} (\widehat{\mathbf{b}}_{i+1} - \widehat{\mathbf{b}}_i)'(\widehat{\mathbf{b}}_{i+1} - \widehat{\mathbf{b}}_i)}{2(m-1)} \right]^{-1} (\widehat{\mathbf{b}}_i - \overline{\mathbf{b}}) \text{ for } i = 1, 2, \ldots, m, \quad (7.5)$$

where

$$\overline{\mathbf{b}} = \frac{\sum_{i=1}^{m} \widehat{\mathbf{b}}_i}{m}. \quad (7.6)$$

7.2 Simulation Study Setup

We now explain the general procedure for the simulation studies used to compare the NL and NLM methods. To generate the multivariate normal errors and random effects we first generated univariate normal data and used the Cholesky decomposition to transform the generated univariate data to multivariate data. The multivariate data are then added appropriately to the nonlinear function to get the generated values of the response variable. The data are fit with separate NL regression models or a NLM model using the nlin and nlmixed procedures of $SAS^{®}$ with the correct model specification.

The control limit is established using the appropriate percentiles of the beta or χ^2 distributions so that the probability of signal for the in-control data is .05, the nominal value. The actual probability of signal is estimated by the proportion of datasets where there was a signal. That is, a signal occurs when at least one of the T^2 statistics exceeds the control limit.

When doing simulation studies with NL and NLM models, the frequency of non-convergence will be much higher than for the LMM. As a result, it becomes more crucial to use good starting values when obtaining the estimates in a NL or NLM model. We found that in general, the more variability there is in the simulated data, either due to increased variability in the errors or larger variance components of the random effects distribution, the more frequent the non-convergence. To reduce the frequency of non-convergence, it is often recommended to use good starting values for the fixed parameters and components of the variance-covariance matrix. The comments of Section 4.7 apply here so we used the known parameter values used to generate the data as starting values of the iterative algorithm.

We note that the regression equivariance discussed in Appendix D that holds for the LMM

does not hold for the NL and NLM models. The unfortunate consequence is the difficulty in obtaining broad conclusions from a smaller set of simulation studies because the obtained results will depend on the type of nonlinear function, its particular form, and the values of its parameters. In order to investigate via simulation the differences obtained by using the NL versus the NLM approach, we picked a nonlinear function related to a real data situation to ensure that our results will hold when analyzing the corresponding dataset. We believe that the conclusions obtained here will hold for other types of functions, but it would be very difficult to make a general conclusion to all functions.

Figure 7.1: Fitted curves for dose response data of Williams et al. (2006a).

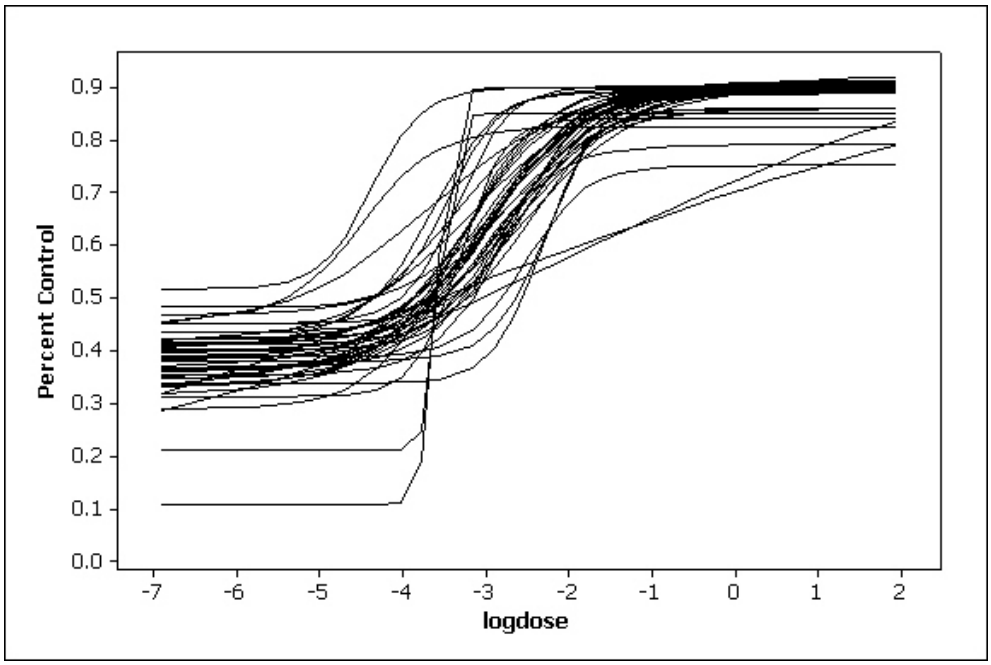

We considered the dose-response data described in Williams et al. (2006a) which can be modeled by the 4-parameter logistic curve mentioned in (6.3) of Chapter 6. The fitted data curves are shown in Figure 7.1. Note that the values for the dose were not equally spaced but the log of the values of the dose were equally spaced.

In considering these dose-response data curves, exploratory data analysis shows that after eliminating several of the profiles due to lack of model fit, the median values of the 4 parameters are very close to $A_i = .9$, $B_i = 2$, $C_i = .05$, and $D_i = .4$. We use this function and its parameter values as typical for this particular application. We also considered the four parameter logistic curve with two other sets of parameter values representing functions more extreme than the median function which we denote the maximum curve and the minimum curve. The maximum curve has parameter values of $A_i = 1$, $B_i = 4$, $C_i = .05$, and $D_i = 0$ and has a steeper rate of change than the median curve with the asymptotes further apart from each other. The minimum curve has parameter values of $A_i = .75$, $B_i = 1$, $C_i = .05$, and $D_i = .5$ and has a more gradual rate of change with the asymptotes closer together.

7.3 Uncorrelated Data with no Random Effects

We first investigated the probability of signal of the method of fitting separate NL regression models as proposed by Williams, Woodall, and Birch (2003). We considered the situation where there are no random effects and the errors are independent. For randomly generated in-control data, we want to determine if the control limit based on beta or χ^2_p distributions is appropriate. Here the data are balanced and equally spaced. Ten thousand datasets were generated for each run of the simulation studies.

Figure 7.2 shows the probability of signal for in-control data generated from both the 4-parameter logistic median and maximum curves. The horizontal axis is the number of observations per profile, n, and the vertical axis is the probability of signal for various values of m and σ^2 for methods based on both $T^2_{1,i,NL}$ and $T^2_{2,i,NL}$. We see that while the methods based on $T^2_{1,i,NL}$ and $T^2_{2,i,NL}$ give similar performance, the probability of signal can be much

Figure 7.2: Probability of signal for two T^2 statistics for simulated in-control data following the median and maximum curve for various values of m, n, and σ^2.

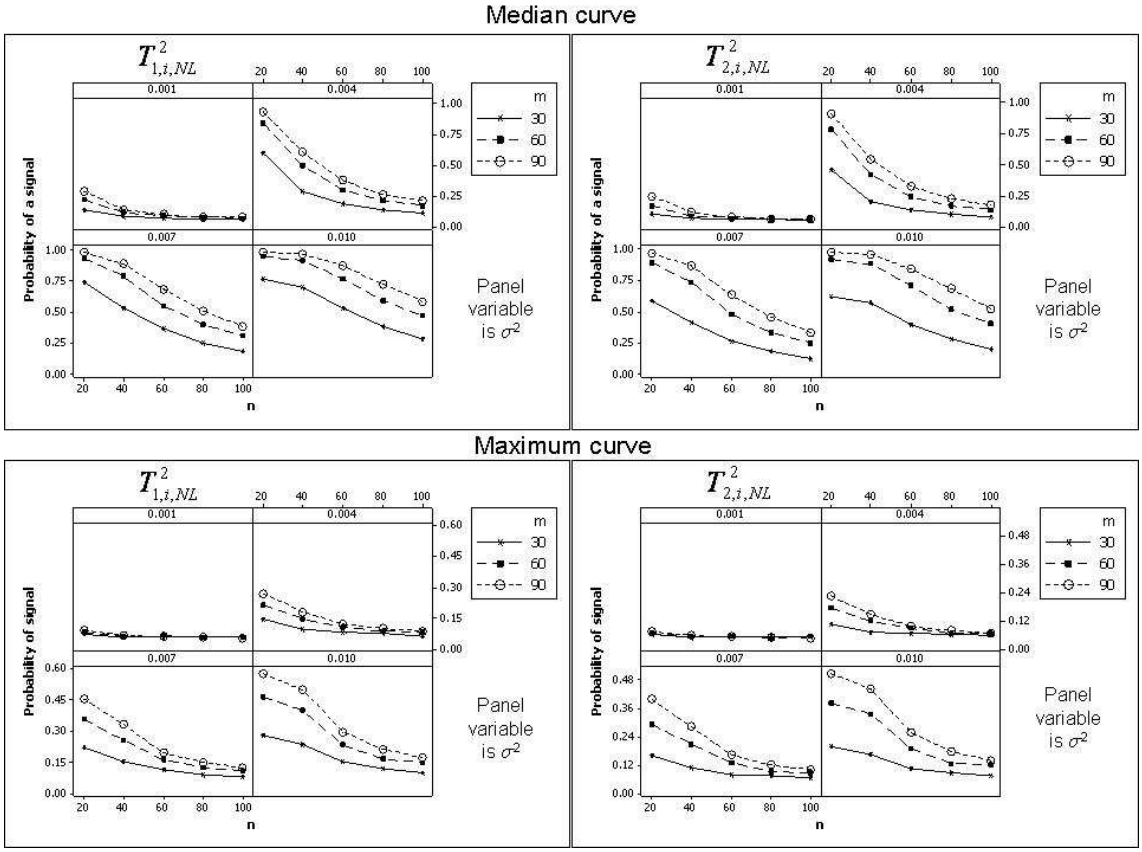

larger than the desired .05 level, particularly as σ^2 increases. When there is little variability in the errors the nominal probability of signal will be maintained.

The probability of a signal decreases as n increases. Thus, if there are more observations per profile, the parameter estimators are more stable and the control limit based on the beta or χ^2_p distributions is appropriate. This is to be expected because the NL model parameter estimators are only asymptotically (in n) normal. Normality is required for the T^2 statistics in (7.1) and (7.3) to have a beta or χ^2_p distribution, respectively. Thus when using a smaller number of observations per profile it is not appropriate to use a control limit that requires

the assumption of normality.

On the other hand, the probability of signal increases when m increases suggesting that when there are more profiles present, it is more likely that at least one of them will be declared an outlying profile than when there are not many profiles present.

Figure 7.3 shows the probability of signal for in-control data generated from the minimum curve. The probability of signal was calculated only for a single, smaller value of $\sigma^2 = .001$, because larger amounts of variability of the errors made the probability of signal virtually 1, and the algorithm had difficulty handling larger amounts of variability without convergence problems.

Figure 7.3: Probability of signal of two T^2 statistic for simulated in-control data following the minimum curve for various values of m and n, with $\sigma^2 = .001$.

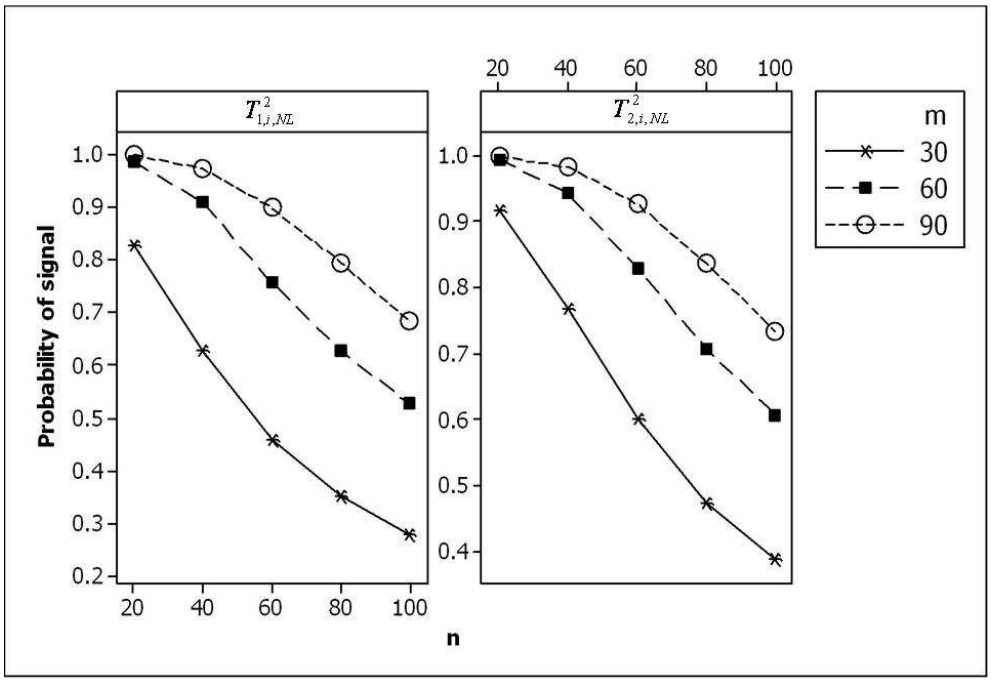

In conclusion, for this particular 4-parameter logistic model, the control limit based on

beta or χ^2_p distributions will not be appropriate for any of the three types considered unless n is sufficiently large and σ^2 is sufficiently small. Results not shown here for other values of A_i, B_i, C_i, and D_i concur with our conclusions here even though it should be noted that because regression equivariance does not hold, there are some situations where the control limit will be sufficiently accurate. Otherwise, the control limit will have to be simulated for practical applications.

It would be possible to consider other data scenarios such as balanced, unequally spaced data or unbalanced data but we do not pursue it here in light of the results obtained for the LMM in Chapter 5. In other words, if the asymptotic control limit is inadequate for balanced, equally spaced data then it will be even more inadequate for data that are unequally spaced, or unbalanced.

7.3.1 Missing Data

Because the asymptotic control limit is inadequate for complete datasets, it will be even more inadequate for profile data that have missing observations within the profile and make the control limit of less use in the NL model. To illustrate, consider Figure 7.4, which shows the probability of signal for $T^2_{1,i,NL}$ and $T^2_{2,i,NL}$ obtained from in-control data generated according to the median curve. Missing data were introduced at random as we did in Section 5.7 and the panel variables are $\%n$ and $\%m$ respectively. The median curve was used here with $m = 30$ and $\sigma^2 = .001$ so the results in Figure 7.4 can be compared with the upper left panel of the median curve graphs in Figure 7.3. We see that increasing amounts of missing data reduce the effectiveness of the control limit and that $\%n$ has a larger impact than $\%m$. It appears that the increase in the probability of signal due to missing data is much larger in the NL approach than in the LS approach as was shown in Figure 5.6 and 5.7.

Figure 7.4: Probability of signal for in-control data with missing observations for $T^2_{1,i,NL}$ and $T^2_{2,i,NL}$ where the panel variables are $\%n$ and $\%m$ respectively. The median curve was used with $m = 30$ and $\sigma^2 = .001$.

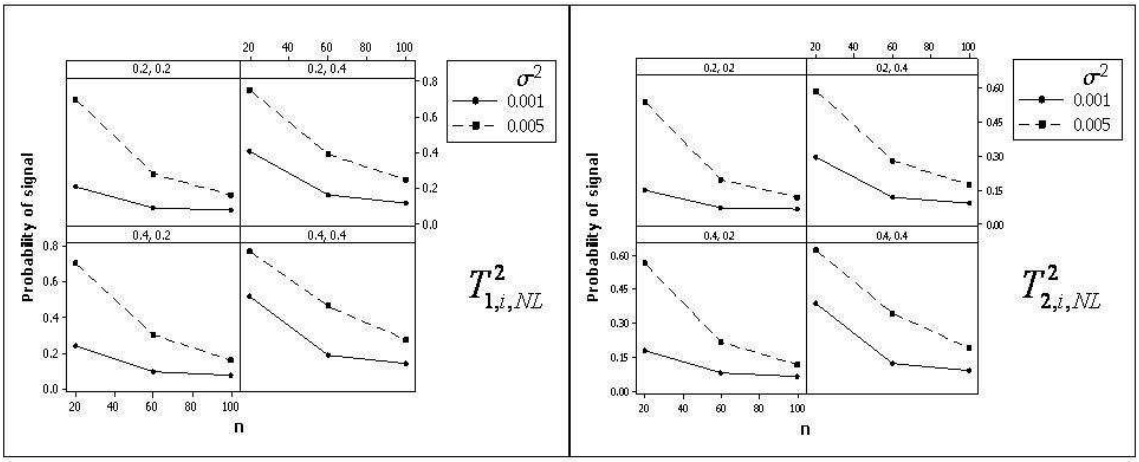

7.4 Uncorrelated Data with One Random Effect

Because of the inherent difficulty in modeling multiple random effects as mentioned in Section 6.3, we next considered data where a single random effect is present. We wish to compare the NL approach with a NLM approach when analyzing the 4-parameter logistic model. To determine which parameter to set at random we analyzed the dose-response data of Williams et al. (2006a) shown earlier in Figure 7.1. After initial data cleaning and testing of lack of fit, there remained 36 profiles for analysis. We calculated the parameter estimates for separate NL regression models for each profile. The mean and variance of the parameter estimates for the 36 profiles are shown in Table 7.1.

It is clear that B_i has the largest amount of variability among the profiles and thus it is the best candidate to be modeled as a random effect in a NLM model. We rewrite (6.3) as

$$y_{ij} = A_i + \frac{D_i - A_i}{1 + \left(\frac{x_{ij}}{C_i}\right)^{B+b_i}} + \epsilon_{ij} \text{ for } i = 1, 2, \ldots, m, j = 1, 2, \ldots, n_i, \tag{7.7}$$

Table 7.1: Mean and variance of the parameter estimates obtained from separate NL models for the dose-response data of Williams et al. (2006a).

Parameter	Mean	Variance
A_i	0.8955	0.0003
B_i	2.0220	0.4300
C_i	0.0525	0.0003
D_i	0.3911	0.0027

where b_i is the random effect that represents how much the slope parameter of the i^{th} profile differs from the overall slope parameter, B.

To determine the values of σ_B^2 that we will use when generating the simulated data, we chose to use values similar in magnitude to the estimated variance of the random effect from Table 7.1. The values for σ_B^2 that we considered were all between .1 and .5 We generated in-control data that followed the median 4-parameter logistic curve with one random effect and uncorrelated errors. In one study, we set $\sigma^2 = .001$ and $\sigma_B^2 = .5$ and performed one thousand simulation runs. Table 7.2 shows the probability of signal when using the approximate control limit for $m = 30$ and various values of n. A smaller number of runs was performed here when modeling the random effect than when there was no random effect because of the larger computational burden required to obtain estimates for the NLM approach.

The NL approach is the wrong approach here because it ignores the random effect, thus we see that the probability of signal for the NL method is quite large and that the NLM method does a much better job of keeping the probability of signal close to the nominal .05 level. Notice that the probability of signal for the NL approach is higher in Table 7.2 than it was for the upper left panel of Figure 7.2. Additional variability in the nonlinear data (due to the random effect) causes the performance of the NL approach to deteriorate. In contrast, the NLM approach does not worsen because it is correctly accounting for the increased

Table 7.2: Probability of signal for the four T^2 statistics for simulated data from a median 4-parameter logistic curve with a single random effect. Here n ranges from 10 to 500, $m = 30$, $\sigma^2 = .001$, and $\sigma_B^2 = .5$.

n	$T^2_{1,i,LS}$	$T^2_{2,i,LS}$	$T^2_{1,i,MIX}$	$T^2_{2,i,MIX}$	Non-convergence in NL	Non-convergence in NLM
10	0.740	0.606	0.070	0.043	0.0216	0.1240
20	0.692	0.586	0.040	0.031	0.0072	0.1245
40	0.681	0.557	0.037	0.033	0.0055	0.1361
50	0.674	0.587	0.038	0.035	0.0051	0.1613
60	0.708	0.585	0.030	0.023	0.0045	0.1670
80	0.685	0.592	0.030	0.017	0.0044	0.1763
100	0.667	0.566	0.036	0.031	0.0039	0.1808
200	0.679	0.581	0.033	0.028	0.0032	0.1737
500	0.676	0.570	0.043	0.028	0.0027	0.1750

variability. As a result the approximate control limit based on the asymptotic normality assumption will not be very accurate for the NL approach when random effects are present. As n increases, the NL method does not improve. This is because the asymptotic results of the NL estimators does not necessarily hold in the presence of random effects. One concern is that the frequency of non-convergence in the NLM method is higher and appears to increase slightly as n increases, nonetheless, the NLM approach is still the preferred approach. The probability of signal calculations for the methods based on $T^2_{1,i,MIX}$ and $T^2_{2,i,MIX}$ statistics shown in Table 7.2 involve only the simulated runs where there was convergence in the parameter estimation.

Now consider how the variability of the random effect impacts the results shown in Table 7.2. We repeated the same simulation study used to generate Table 7.2 with different values of σ_B^2 used to generate the data. Figure 7.5 shows the probability of signal for the T^2 statistics for different values of σ_B^2 where $m = 30$ and $\sigma^2 = .001$. Figure 7.6 shows the proportion of

non-convergence of the NLM approach as σ_B^2 varies where $m = 30$ and $\sigma^2 = .001$.

Figure 7.5: Probability of signal for $T^2_{1,i,LS}$, $T^2_{2,i,LS}$, $T^2_{1,i,MIX}$, and $T^2_{2,i,MIX}$ for in-control data for the median curve where σ_B^2 varies from .1 to .5. In this case $m = 30$ and $\sigma^2 = .001$.

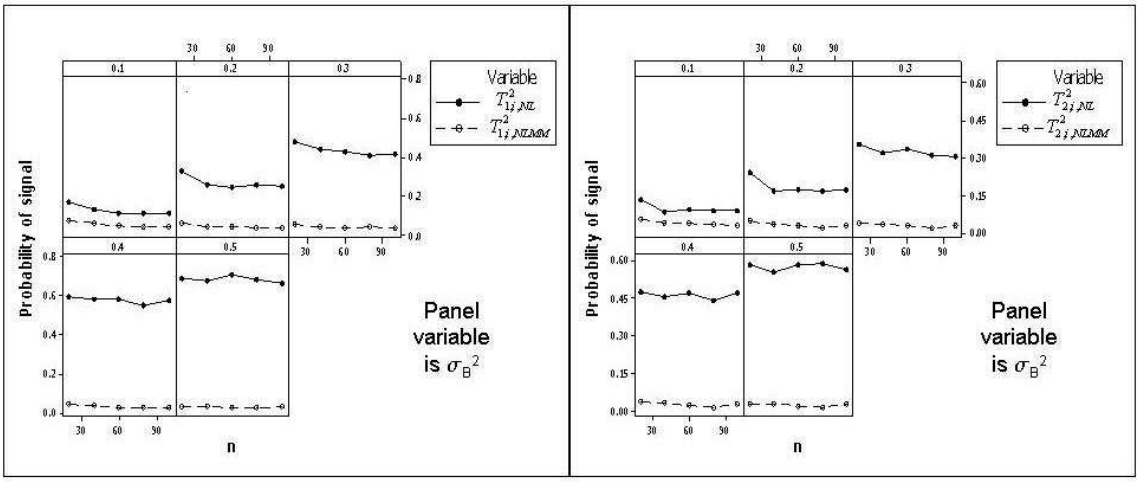

From Figure 7.5 we see that as the variability of the random effect gets smaller, the difference between the NL and NLM methods nearly disappears. This is because as σ_B^2 decreases, the profiles are more similar to each other and the more similar they are to profiles with no random effects. In addition, in Figure 7.6 we see that the proportion of non-convergence decreases as σ_B^2 decreases. There are slight increases in the proportion of non-convergence as n increases, likely due to the increased computational difficulty for increased sample sizes.

We do not show specific results where σ^2 changes but note that its impact on data with random effects is the same as the impact on uncorrelated data with no random effects as was shown earlier in Figure 7.2. That is, increasing σ^2 will increase the probability of signal for the NL approach with in-control data. We chose a smaller value of σ^2 for the results in this section, resulting in a smaller probability of signal for the NL method, in order to illustrate the impact of changing σ_B^2.

Figure 7.6: Proportion of non-convergence in NLM approach for the median curve when $m = 30$, $\sigma^2 = .001$ and n and σ_B^2 vary.

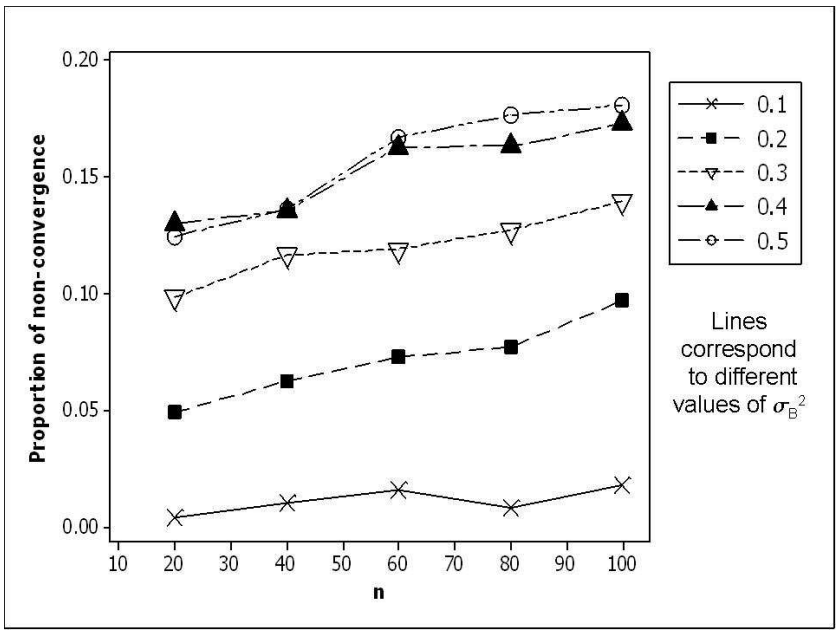

To illustrate the out-of-control performance of the NL and NLM methods we did power studies similar to those of Chapter 5 for the LMM. With the 4-parameter logistic curve, a shift in the profiles can be introduced in any of the 4 parameters. We considered a step shift in B which represents a change in the steepness of the profiles. Figure 7.7 shows the out-of-control performance for the median curve with $T^2_{2,i,NL}$ and $T^2_{2,i,NLMM}$ when there is an increase in B after the fifth profile. Here $m = 30$, $\sigma^2 = .001$, n varies from 10 to 60, and the value of B increases by values ranging from 0 (the in-control case) to 5. We do not show the results for methods based on $T^2_{1,i,NL}$ nor $T^2_{1,i,NLMM}$ because they have little ability in detecting step changes as demonstrated by Sullivan and Woodall (1996). To obtain these results in Figure 7.7, the control limit was simulated in order to ensure that the probability of signal for in-control data is equal to .05. One thousand datasets were simulated to generate the power curves.

Figure 7.7: Probability of signal for $T^2_{2,i,NL}$ and $T^2_{2,i,NLMM}$ for out-of-control data for the median curve where σ^2_B and n vary. Here $m = 30$ and $\sigma^2 = .001$ and the step change in B occurred after the fifth profile.

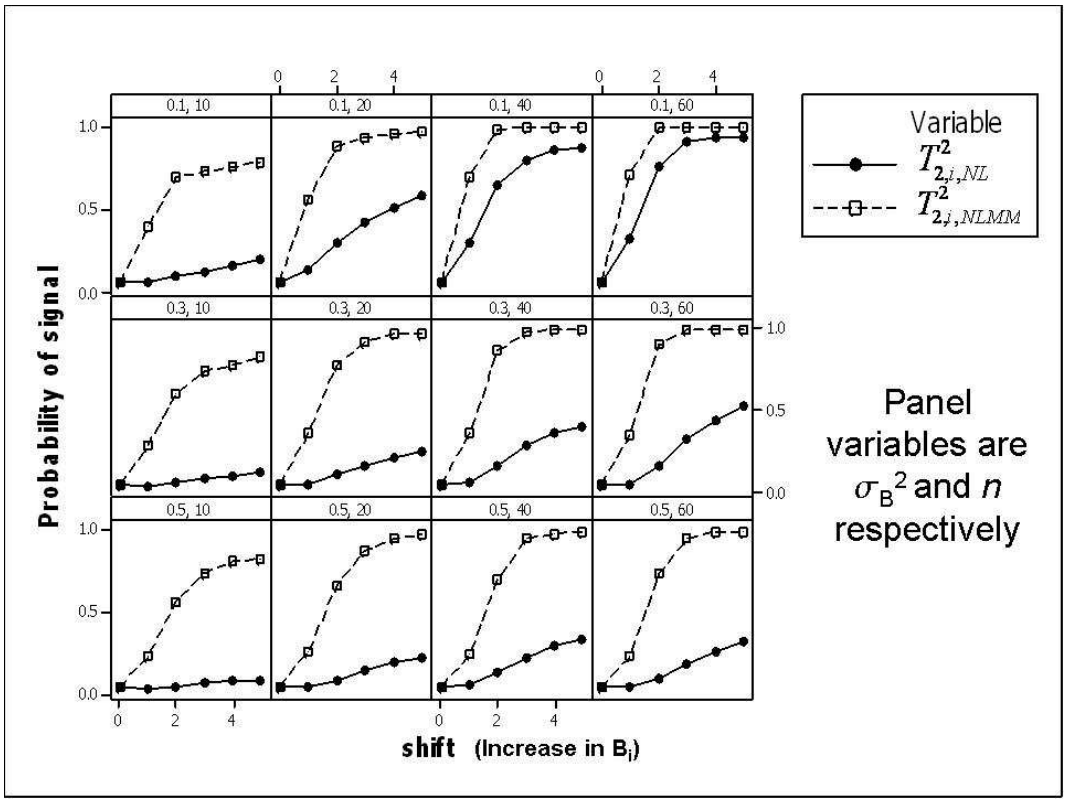

We see that the NLM approach clearly has a much higher probability of detecting the change than the NL approach. The difference for the two approaches is larger when σ^2_B is larger because the difference between the power curves is larger for the bottom row of Figure 7.7 than for the top row. This is because the NLM approach is taking into account the larger variability in the random effect that the NL approach ignores. As n increases, the closer the two approaches will be because they are both fitting the nonlinear curves equally well. When there is a smaller number of observations per profile, the NL approach will not fit the curves as well whereas the NLM approach pools information together across profiles to achieve a better fit. As an added bonus and not shown here, we found that the frequency

of non-convergence decreased for the NLM as the size of the shift increased. Similar results were obtained for the maximum and minimum curves, thus they are not presented here.

We do note that there is a dependence of the results on the location of the shift. Figure 7.8 shows the probability of signal for out-of-control data from the median curve for $m = 30$, $n = 20$ and when the step change occurred at different locations. We see that the NLM approach is always at least equivalent to the NL approach and often times far superior. The closer the shift is to the beginning of the data collection procedure the better the NLM approach will be.

Figure 7.8: Probability of signal for $T^2_{2,i,NL}$ and $T^2_{2,i,NLMM}$ for out-of-control data from median curve for various locations of the step change where there is an increase in B. Here $m = 30$, $n = 20$, $\sigma^2_B = .1$ and $\sigma^2 = .001$.

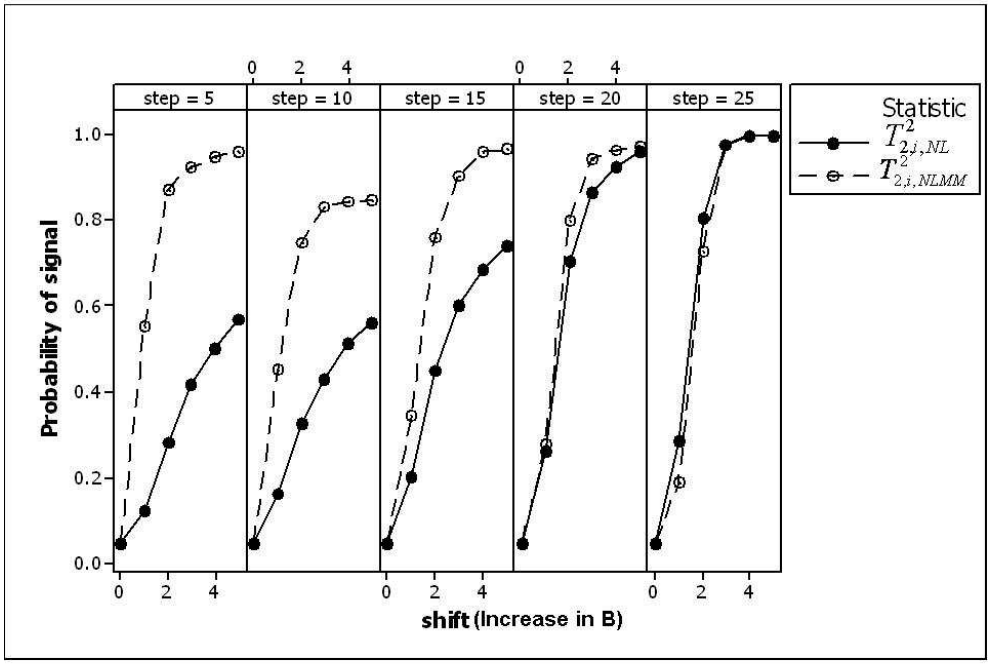

To explain the dependence on the locations of the shift, recall that because of regression

equivariance, the appropriateness of the approximate control limit depends on the values of the parameters used in the function. For example, notice from Figure 7.2 that the probability of signal for the NL approach is different for the maximum curve than for the median curve. For each of the different locations where the step change occurs, there is a different mix of curves with different parameter values, thus the difference between the NL and NLM approaches is not the same across all values of the step change.

This lack of regression equivariance makes it difficult to generalize the conclusions regarding the increases to what occurs when there are decreases in B. To illustrate, compare Figure 7.8 with Figure 7.9 which shows the probability of signal for decreases in B. An issue to be concerned with when studying decreases in B is that when B value is close to zero, the greater the chance that there will be instability in the numerical algorithms used to obtain the results. Thus the generated curves used in Figure 7.9 are the same as the median curve used to generate Figure 7.8, except that the in-control value of $B = 7$ instead of 2. We see again that the probability of signal depends on the location of the shift. In Figure 7.9, the difference between the NL and NLM approaches is largest for later shifts and negligible for earlier shifts. Note that the results for step=5 in Figure 7.8 are similar to the results for step=25 in Figure 7.9. This is because in the first case when step=5, the in-control curves are equivalent to the out-of-control curves from the second case and vice versa.

7.5 Correlated Data With Random Effects

Now consider the situation where the profiles have correlated errors with random effects but still are balanced and equally spaced. In our review of the literature on the NLM model, we found that the $\mathbf{R}_i$ matrix is often assumed to be a diagonal or identity matrix, a fact

Figure 7.9: Probability of signal for $T^2_{2,i,NL}$ and $T^2_{2,i,NLMM}$ for out-of-control data for various locations of the step change where there is a decrease in B. Here $m = 30$, $n = 20$, $\sigma^2_B = .1$ and $\sigma^2 = .001$.

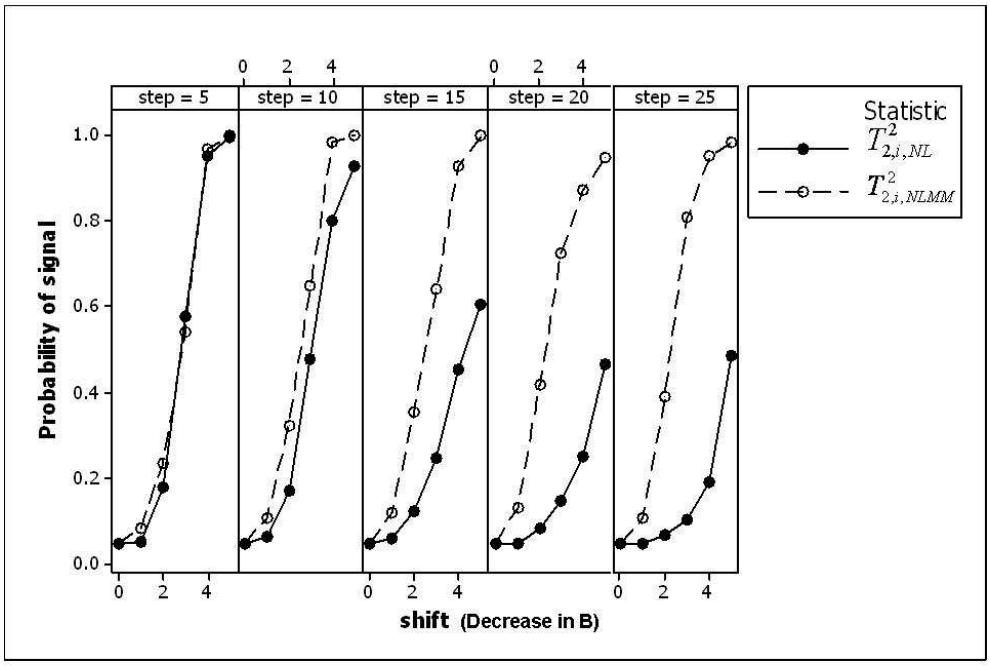

also noted by Davidian and Giltinan (2003). This is because the variability between profiles represented by the random effects has a bigger impact on the variability in the response than does the correlation within profiles. This was noted for the linear mixed model by Verbeke and Molenbergs (2000) and for the NLM model by Davidian and Giltinan (1995, 2003). As a result software such as $SAS^{®}$ and S-Plus do not allow specification of a correlation structure of the errors in conjunction with integral approximation methods although they do allow for correlation with linearization methods (Schabenberger and Pierce, 2002, p. 538).

In addition, it was noted by Schabenberger and Pierce (2002) that modeling the correlation concurrently with a random effect makes little difference in the results obtained but can increase the likelihood of convergence problems. To model the correlation in the NLM

Table 7.3: T^2 statistics for the NL and NLM approaches for data with uncorrelated and correlated errors. The generated data follow the median curve with $m = 30$, $n = 20$, $\sigma_B^2 = 0.5$ and $\sigma^2 = .001$.

ρ	$T^2_{1,i,NL}$	$T^2_{2,i,NL}$	$T^2_{1,i,NLMM}$	$T^2_{2,i,NLMM}$
0.0	0.6784	0.5680	0.0502	0.0378
0.1	0.6766	0.5642	0.0470	0.0366
0.2	0.6810	0.5660	0.0428	0.0336
0.3	0.6836	0.5706	0.0404	0.0295
0.4	0.6786	0.5638	0.0360	0.0288
0.5	0.6742	0.5602	0.0310	0.0277
0.6	0.6716	0.5594	0.0292	0.0263
0.7	0.6542	0.5498	0.0275	0.0258
0.8	0.6358	0.5286	0.0302	0.0279
0.9	0.6226	0.5090	0.0433	0.0332

approach would be difficult in practice. It would require one to program the numerical algorithms to obtain the estimates because they are not readily available in $SAS^{®}$ or S-Plus when using the integral approximation approach. Thus, although theoretically possible, it is not easy to obtain a NLM model fit with correlated errors. We present here empirical evidence showing that it may be sufficient to simply model the random effects and not model the correlation in our application.

For the median 4-parameter logistic curve we generated in-control data with uncorrelated and correlated errors where there was a single random effect in B_i. In Table 7.3 we show the probability of signal for the T^2 statistics based on the NL and NLM approaches for in-control data following the median curve with $m = 30$, $n = 20$, $\sigma_B^2 = 0.5$ and $\sigma^2 = .001$ and where different amounts of correlation were introduced in the errors. There is a large difference in the probability of signal for the T^2 statistics based on the NL approach when compared to those based on the NLM approach, but there is little difference in the T^2 statistics as the amount of correlation in the errors increases. Thus the modeling of the random effect has a

large impact on the appropriateness of the control limit.

Figure 7.10: Probability of signal for $T^2_{2,i,NL}$ and $T^2_{2,i,NLMM}$ for out-of-control data following the median curve where a step change occurred after the fifth profile. Here $m = 30$, $\sigma^2_B = 0.5$ and $\sigma^2 = .001$.

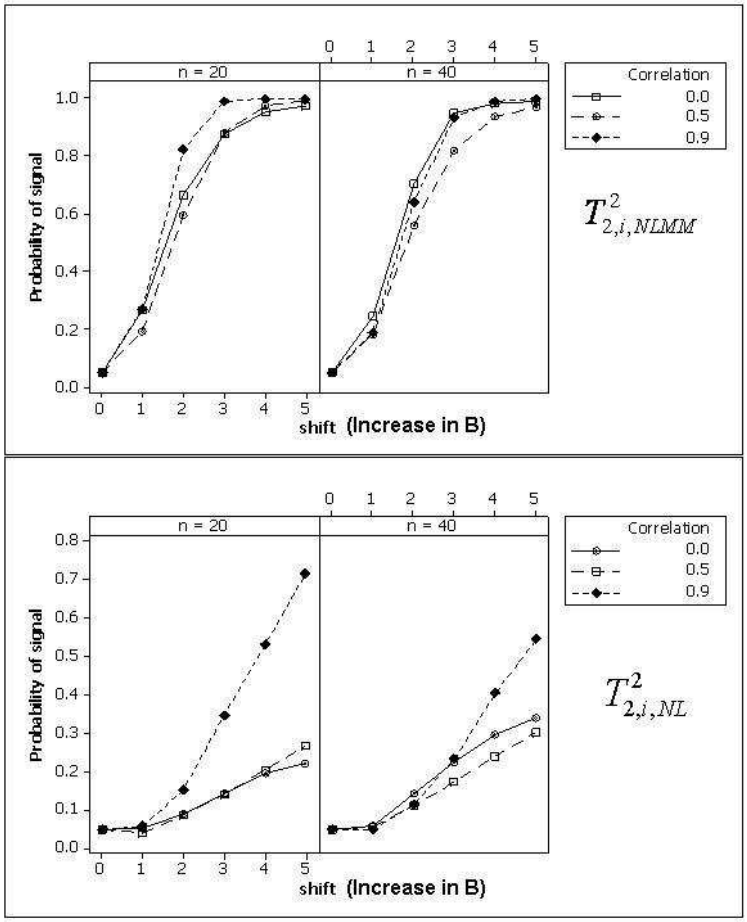

When considering the out-of-control case as done previously, we show in Figure 7.10 the probability of signal for the methods based on $T^2_{2,i,NL}$ and $T^2_{2,i,NLMM}$ when a step change was introduced in the profiles when the data have uncorrelated or correlated errors. We see that the NLM approach gives us a higher probability of signal than the NL approach across the levels of correlation.

We noted in Chapters 4 and 5 that we could model the correlation of the errors in the

LMM and included references where it was recommended to model both levels of correlation. In contrast, to summarize the results here, we see that the NLM approach that ignores the correlation in the errors is superior to the NL approach even when the errors are correlated. We note that this does not mean that we could not do even better with a NLM approach that does model the correlation in the errors. While we do not believe the NLM approach could be improved drastically by explicitly modeling the correlated errors, it remains to be seen how much improvement could be gained.

7.6 Proposed Method

Our proposed method of Phase I analysis when considering nonlinear profiles uses both the NL and NLM to determine outlying profiles. It builds on the approach of Williams et al. (2006a) who proposed the following steps:

1. If there is replication of the points taken at each location along the profile, then the homogeneity of variance can be checked. Profiles that do not have a homogeneous variance across the locations within the profile are eliminated from the dataset after inspecting the appropriate T^2 statistic, which is obtained by using a variance regression model.

2. Determine the appropriateness of the choice of the nonlinear function through a lack-of-fit (LOF) test. This test can be performed whether or not there is replication of the points although when there is no replication, the lack-of-fit test is model based.

3. Fit separate NL regression models to each of the profiles to obtain individual profile parameter estimates. Use the estimates for the basis of the T^2 statistics as in (7.3). This step corresponds to the NL approach studied earlier.

Our approach uses the first two steps of the approach outlined above and replaces step 3 with two new steps that utilize the NLM model. Thus the last two steps of our proposed approach are given by:

3. Fit separate NL regression models to each of the profiles to obtain individual profile parameter estimates. Compute the sample variances across the m profiles for each of the parameters. Upon inspecting the sample variances for large values relative to the other values, determine which parameters, if any, should be modeled with random effects, trying to keep the number of random effects small. In many cases, there will be one or two of the nonlinear parameters that have much larger variability than the others; these should be prime candidates for inclusion of random effects.

4. Fit the NLM model using the determination of random effects from the previous step to obtain the predicted random effects. Use the predicted random effects as the basis for the T^2 statistics to determine outlying profiles as in (7.5). The control limit can be obtained by using the corresponding percentiles of the appropriate distribution. This step corresponds to the NLM approach studied earlier and compared with the NL approach.

This proposed approach will be illustrated in the examples that follow in the next two sections. We present one example with replicated data observations and one without replication.

7.7 Example with Replicated Data Observations

To illustrate the proposed method when the data observations for a profile have replicate measurements at each location, we use the dose-response data of Williams et al. (2006a) that has been discussed previously. The original dataset had 44 profiles, each of which had 4 replicates measurements at 8 different locations. The fitted profiles from separate NL regression models were shown in Figure 7.1.

The first two steps of our proposed method were performed by Williams (2005) and resulted in the elimination of 8 profiles due to lack of fit and lack of homogeneity of variance. For the third step the mean and variance of the remaining 36 profiles were calculated previously and shown in Table 7.1. We conclude that a single random effect in B is appropriate. The final step is to fit the NLM model with the random effect in B. Figure 7.11 shows the control chart based on the NLM model and Figure 7.12 shows the control chart that would be done according to the approach of Williams et al. (2006a).

Figure 7.11: T^2 control charts for the NLM approach for the dose response data of Williams et al. (2006a).

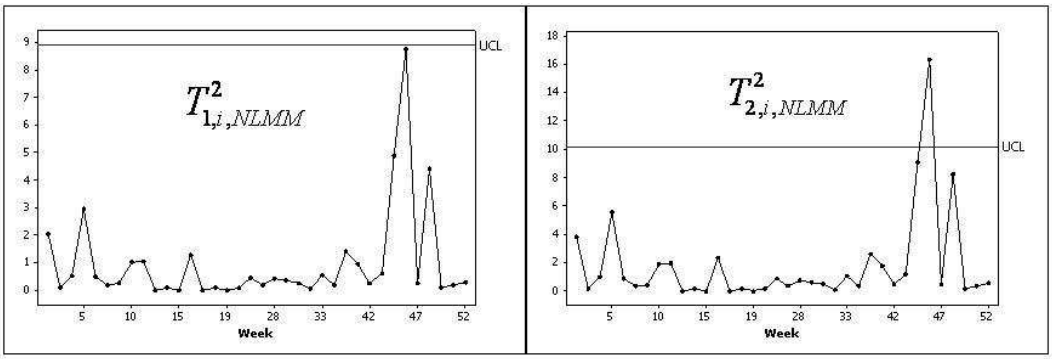

There are slight differences in Figures 7.11 and 7.12. We see that using the NLM model approach gives one fewer signal than does the NL approach for both versions of the T^2

Figure 7.12: T^2 control charts for the NLM approach for the dose response data of Williams et al. (2006a).

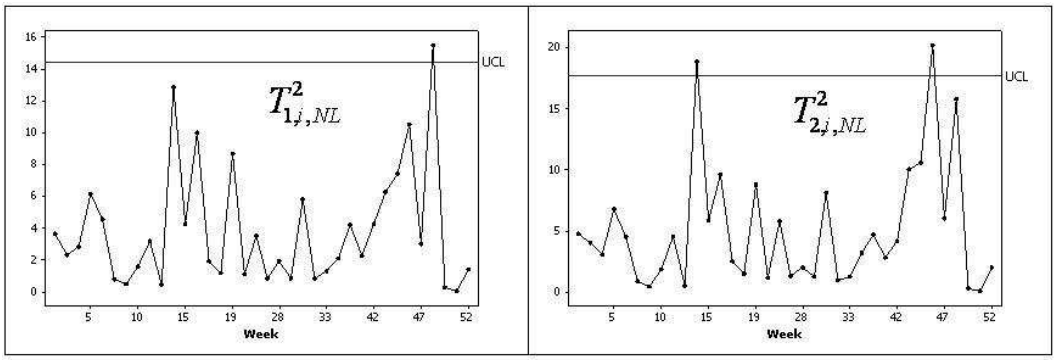

statistic. Based on the earlier simulation results of this chapter, the NL approach would give too many signals while the NLM approach preserves the appropriate probability of signal. While it is not known whether or not the underlying process truly had outliers or not, we are more confident in the charts of Figure 7.11 and would eliminate the profile corresponding to week 46 prior to proceeding to Phase II.

7.8 Example with Unreplicated Data Observations

The second example that we use to illustrate the differences between the proposed approach and the approach of Williams et al. (2006a) is the particle board data presented in Walker and Wright (2002) and studied by Williams, Woodall, and Birch (2003). In the initial analysis, there were 24 boards, each of which had 314 measurements along the profile. There is only a single measurement at each location so there will be some adjustment of our proposed method. The raw data profiles are shown in Figure 7.13.

Williams, Woodall, and Birch (2003) fit a nonlinear function requiring six parameters

Figure 7.13: Raw data profiles for the particle board data of Walker and Wright (2002).

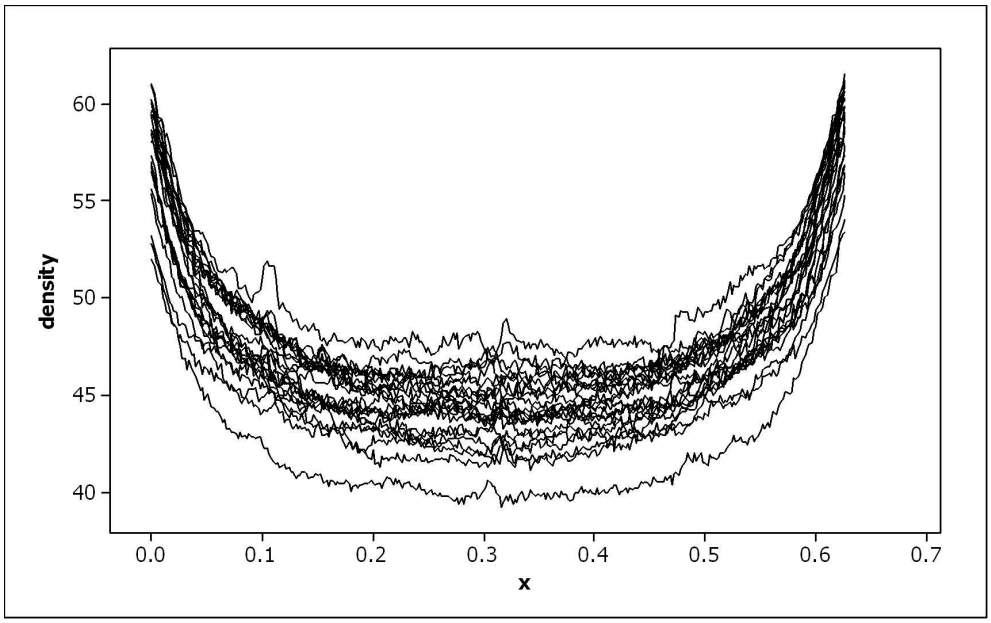

(a "bathtub" function) to the raw data profiles. These parameters consisted of a lower asymptote, the center where the lower asymptote is achieved and four other parameters determining the flatness of the center of the curve and the rate at which the curve increases. This allows the curve to be asymmetric about the center. The model can be written as

$$y_{ij} = \left\{ \begin{array}{c} E_{1,i}\left(x_{ij} - H_i\right)^{F_{1,i}} + G_i \text{ if } x_{ij} > H_i \\ E_{2,i}\left(-x_{ij} + H_i\right)^{F_{2,i}} + G_i \text{ if } x_{ij} \leq H_i \end{array} \right\} \text{for } i = 1, 2, \ldots, m, j = 1, 2, \ldots, n_i, \quad (7.8)$$

where $E_{1,i}$, $E_{2,i}$, $F_{1,i}$ and $F_{2,i}$ represent the rate of increase and flatness in the profiles, G_i is the lower asymptote, and H_i is the center point where the curve attains the lower asymptote.

Because there is no replication of the points for the locations along the profile, we cannot do the classical test of homogeneity of variance or test of lack of fit that was discussed in Williams (2005). However, because we have multiple profiles we can use the the values across the profiles to determine the viability of the test of homogeneity assumption and whether or

not there is lack of fit.

To check for homogeneity and lack of fit, we use the residuals of the profiles from the separate nonlinear regression models. They are given by

$$r_{ij} = y_{ij} - \widehat{y}_{ij} \text{ for } i = 1, 2, \ldots, m, j = 1, 2, \ldots, n_i, \tag{7.9}$$

where $\widehat{y}_{ij}$ is the predicted value of the nonlinear function using the parameter estimates obtained from separate NL regression model in (6.1). If homogeneity of variance is a valid assumption, then a plot of the residuals versus the measurement location should show residuals with a similar spread across the location. The plot of residuals versus the location for the particle board data is shown in Figure 7.14.

Figure 7.14: Plot of the residuals versus the locations for the particle board data of Walker and Wright (2002) to check homogeneity of variance and lack of fit for the 6-parameter bathtub function.

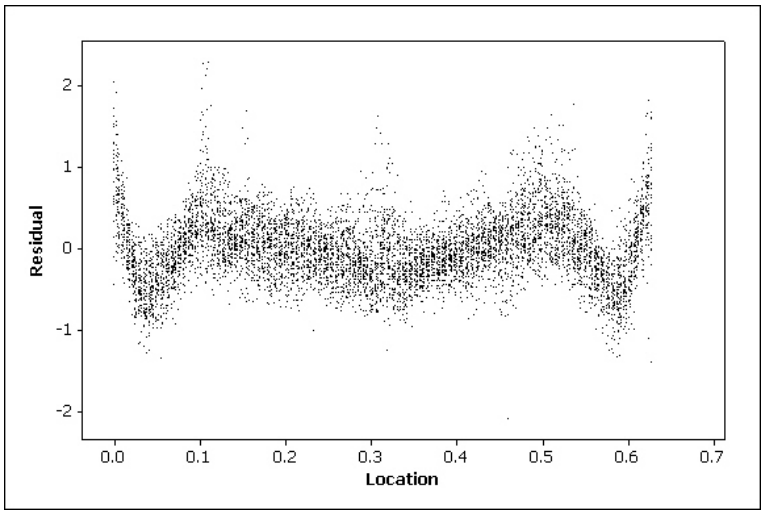

Figure 7.14 shows that the model in (7.8) lacks fit. It is not clear what alternative parametric model could be used to adequately describe the remaining unexplained variability and a non-parametric model may be an appropriate alternative. To examine the homogeneity

of variance, we show in Figure 7.15, boxplots of the residuals shown in Figure 7.14, where the median of each location has been subtracted so that the boxplots are centered at their medians. Subtracting the median removes the lack of fit apparent in Figure 7.14 and allows one to view more clearly the viability of the homogeneity of variance assumption. The variance across the locations in Figure 7.15 appears to be heterogeneous although this may be due to outlying observations within profiles. One potential drawback to the graphs shown in Figures 7.14 and 7.15 is that if there is lack of fit in a single profile, it is difficult to determine which profile could be eliminated to remedy the situation.

Figure 7.15: Plot of the standardized residuals versus the locations for the particle board data of Walker and Wright (2002) to check homogeneity of variance for the 6-parameter bathtub function.

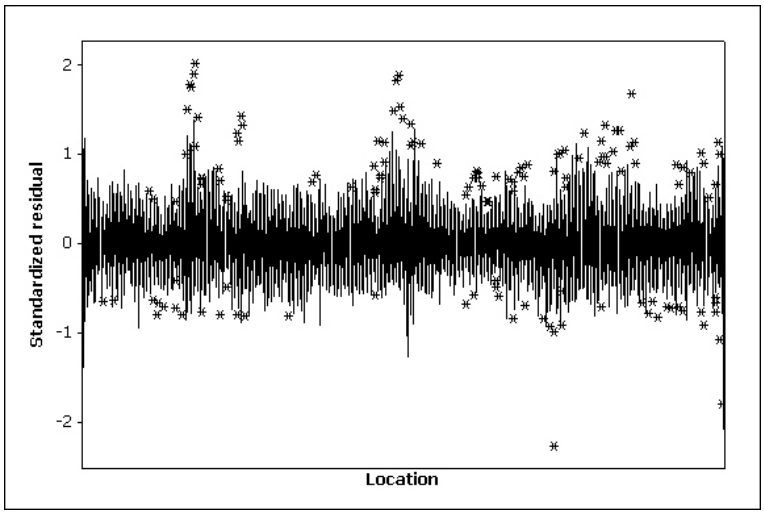

For purposes of illustration, we will show the remainder of the analysis ignoring the lack-of-fit and heterogeneity of variance. Williams (2005) discussed a test for a "lack of consistency" among the m profiles but we do not pursue it here.

Another alternative to test for lack of fit is to divide the points along the profile into different groups and treat the points within a group as "pseudo-replicates". This idea is

discussed in Su and Yang (2006) and its references. We do not pursue this idea here because the particle board data does not lend itself to natural groups within the profile.

Table 7.4: Mean and variance of the parameter estimates for the particle board data of Walker and Wright (2002).

Parameter	Mean	Standard Deviation
$E_{1,i}$	5173	6.445×10^7
$E_{2,i}$	10752	6.958×10^8
$F_{1,i}$	4.293	1.417
$F_{2,i}$	5.128	3.843
G_i	44.425	3.037
H_i	0.2956	0.0017

The third step is to fit the separate NL models and obtain the parameter estimates to determine which random effects to include. The mean and standard deviation of the parameter estimates of the separate NL fits for the particle board data are shown in Table 7.4. We see that the variability of $E_{1,}i$ and $E_{2,i}$ are much larger than any other parameter. Thus they are the most likely candidate for having a random effect.

The final step is to fit the NLM model and obtain the T^2 statistics from (7.4) and (7.5). The resulting charts for the T^2 statistics based on the NLM model is shown in Figure 7.16. One should compare Figure 7.16 with Figure 7.17 which shows the charts obtained for the separate NL regression models from (7.1) and (7.3) and which corresponds to the method of Williams et al. (2006a). We see that the use of charts based on $T^2_{2,i,NL}$ and $T^2_{1,i,NL}$ produce a signal whereas the charts based on $T^2_{2,i,NLMM}$ and $T^2_{1,i,NLMM}$doesn't produce any signals. Thus we conclude that we can use all 24 profiles to obtain the parameter estimates on which the Phase II control charts will be based.

Figure 7.16: T^2 control charts for the NLM approach for the particle board data of Walker and Wright (2002).

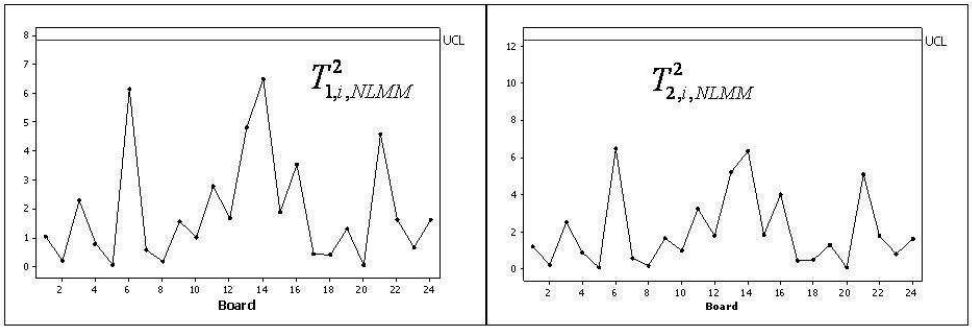

Figure 7.17: T^2 control charts for the NL approach for the particle board data of Walker and Wright (2002).